Electrically Coupled Chemical Oscillators and Their Action Potentials

W. Hohmann, N. Schinor, M. Kraus, and F. W. Schneider*

Institute of Physical Chemistry, University of Würzburg, Am Hubland, D-97074 Würzburg, Germany

Received: April 14, 1999

Electrical coupling of chemical oscillators is shown to be a versatile and rapid method to study the propagation of action potentials (spikes, oscillations) using three, four, and six electrically coupled continuous flow stirred tank reactors (CSTR). Starting with a prepared excitable steady state close to a SNIPER bifurcation in the Belousov−Zhabotinsky (BZ) reaction, conditions are specified for the initiation and propagation of these action potentials in a linear array of reactors and in a cyclic array. In the cyclic array, traveling waves of action potentials were measured for the first time. The coherence and incoherence of two, three, and four chemical BZ oscillators which were mutually electrically coupled was also studied. Numerical simulations with the seven-variables Montanator are in fair agreement with the experimental results.

Introduction

It has been abundantly shown that synchrony (or coherence) is the most common state between coupled "biological oscillators" as seen, e.g., in the synchronous blinking of colonies of glow worms.[1] Interestingly, the difference between certain animal gates has been described by the differences in coupling strength between neurons in a postulated neural generator consisting of coupled oscillators.[2] Generally speaking, synchrony between many coupled oscillators is the rule rather than the exception if the variance of their frequency distribution is not too great and if coupling is sufficiently strong. Excitability and synchrony also play an important role in the recognition of odors in the olfactory neural system of the locust.[3] Thus, a study of excitability in chemical systems may help to better understand the phenomenological features of their biological counterparts.

The coupling of chemical oscillators has been studied extensively. It may be implemented either by convective (passive) mass exchange[4] or by pumping of the reactive contents from one reactor into another (active mass exchange).[5] A further form is flow rate coupling[6] where the flow rate of reactant solutions into the individual reactors becomes a very sensitive bifurcation parameter. In our own work, flow rate coupling has been carried out in early feedback studies with and without time delay using single or serially coupled reactors.[6] Although general mass coupling is quite effective, it has a major disadvantage: only an attractive type of coupling is possible, which means that strong mass coupling always leads to identical dynamic states (either all oscillatory or all steady states but not mixed). Importantly, attractive coupling of two oscillators produces in-phase coherence. On the other hand, repulsive coupling prevents in-phase coherence in the case of coupled oscillatory states. Attractive as well as repulsive coupling is necessary to carry out general recognition processes of patterns in a Hopfield type reactor network[7] in which transitions may occur in both directions, namely, from oscillatory to steady states and vice versa. For this reason, we have employed electric coupling[8] in recognition experiments in reactor networks[7,9−11] by applying an electric potential to Pt-working electrodes which are immersed in the reactors where redox reactions take place. Since electric currents (and electric potentials) can be added as well

as subtracted, positive (attractive) and negative (repulsive) coupling is now possible in a flexible way.

In recent work, we found that the application of an electric current to a Pt-working electrode causes a transition from an oscillatory to a nodal steady state in the Belousov−Zhabotinsky (BZ) reaction mainly involving the Ce^{3+}/Ce^{4+} redox couple.[11] This transition is termed as a SNIPER[12] bifurcation whose nodal steady state is excitable. A pulse (i.e., a reversible crossing of the threshold from the nodal steady state to the oscillating region and back) generates a large response similar to action potentials of in vivo neurons. These responses (action potentials) to electrical pulses may propagate in arrays of electrically coupled reactors (excitators) as studied by passive mass coupling by Marek and co-workers.[13,14]

In the following, we demonstrate the method of electric coupling in linear and cyclic arrays of chemical reactors and we present new experiments which include the observation of sustained traveling waves in a cyclic network of coupled excitators as well as the easy synchronization and phase behavior of mutually coupled chemical BZ oscillators.

Experiment and Procedure

Two (and up to six) plexiglass CSTRs have been electrically coupled (as shown in Figure 1). Each CSTR (volume 4.2 mL) contains a Pt-working electrode ($\sim$2.0 cm^2), a monitoring Pt|Ag|AgCl redox electrode, and a magnetic stirrer (600 rpm). The output of the monitoring Pt|Ag|AgCl redox electrode is termed as an action potential. A Teflon membrane connects each CSTR with its own reference half cell which also contains a Pt working electrode and sulfuric acid (0.4 mol/L). Three reactant feed streams into each CSTR are delivered by precise piston pumps with three syringes containing the following solutions: syringe I, $NaBrO_3$ (0.42 mol/L); syringe II, $Ce_2(SO_4)_3$ (1.5 × 10^{-3} mol/L), malonic acid (0.9 mol/L); syringe III, sulfuric acid (1.125 mol/L). The reactants enter through the bottom of a reactor and the contents flows out at the top. Reactors, feedlines, and syringes are thermostated (25 °C). The redox potentials Pot_i in $CSTR_i$ are digitally monitored (at 1 Hz). Due to variations in the sensitivities of the redox electrodes, the redox potentials are normalized and presented in arbitrary units. A galvanostat (E&G Instruments) delivers a defined current G_i to the Pt
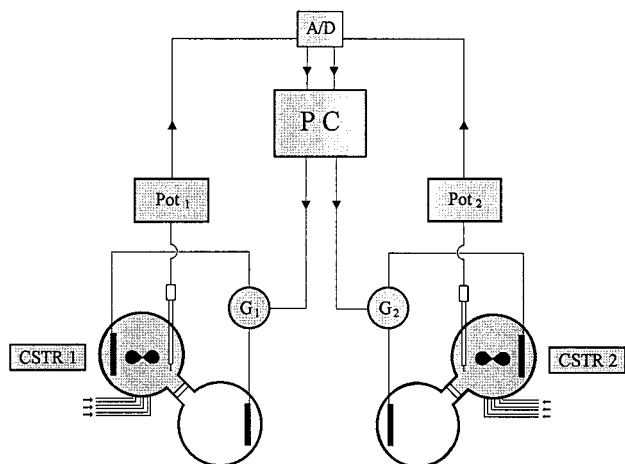
Electrically Coupled Chemical Oscillators

J. Phys. Chem. A, Vol. 103, No. 29, 1999 **5743**

Figure 1. Two CSTRs are connected to their reference compartments via a Teflon membrane. The reactor potentials Pot_i are monitored by Pt|Ag|AgCl redox electrodes, G_i are the electric currents applied to the Pt-working electrodes by galvanostats; A/D, analogue to digital converter; electrical coupling in reactor arrays (two, three, four, and six reactors) is achieved according to eqs 1–5.

working electrode in each CSTR. The CSTRs contain the cathodes, while the reference cells are used as the respective anodes.

Flow Rate as a Bifurcation Parameter in the Absence of an Electric Current. The bifurcation diagram for a single reactor is well-known for the flow rate as a bifurcation parameter.[15] For the above concentrations, oscillations exist in a certain k_f range (from 2.5×10^{-4} s^{-1} to 10.0×10^{-4} s^{-1}). Three Hopf bifurcations occur (at $k_f = 2.5 \times 10^{-4}$ s^{-1}, $k_f = 10.0 \times 10^{-4}$ s^{-1} (secondary Hopf bifurcation), and $k_f = 12.5 \times 10^{-4}$ s^{-1}) with the respective focal steady states. For all experiments, the in-flow concentrations and the flow rates into each CSTR are fixed (6.0×10^{-4} s^{-1} corresponding to a mean residence time of 27.8 min) to obtain the same oscillatory state (period $T = 33$ s) in each reactor in the absence of an electric current.

Electric Current as a Bifurcation Parameter: SNIPER Bifurcation. When an increasing cathodic current is applied to an oscillatory state of the BZ reaction (at $k_f = 6.0 \times 10^{-4}$ s^{-1}), the oscillation frequency decreases and the oscillation amplitude abruptly disappears and gives way to a nodal steady state of lower redox potential (1000 au) at 0.85 mA, where the frequency of the oscillation has reached zero (Figure 2).[11] This point is called a SNIPER (saddle node infinite period) bifurcation. Here a limit cycle collides with a saddle node leading to an oscillation of "infinite" period at the SNIPER point.[16] The nodal steady state is termed as excitable; that is, a sufficiently large (negative) electric pulse (a short removal and reapplication of the current) will cause a single (large amplitude) oscillation (action potential) of the redox potential, as monitored by the immersed Pt-redox electrode. A subsequent pulse will produce the next oscillation only after the characteristic refractory time ($\sim$40 s) has elapsed.

To establish the same nodal steady state in each reactor, a constant bias (1.2 mA) is applied to all Pt-working electrodes. The resulting identical excitable steady states serve as the reference states, and a single chemical reactor may be termed as an "excitator".

Results

Linear Coupling. *Four Excitators.* When four reactors in excitable nodal steady states are coupled unidirectionally, the
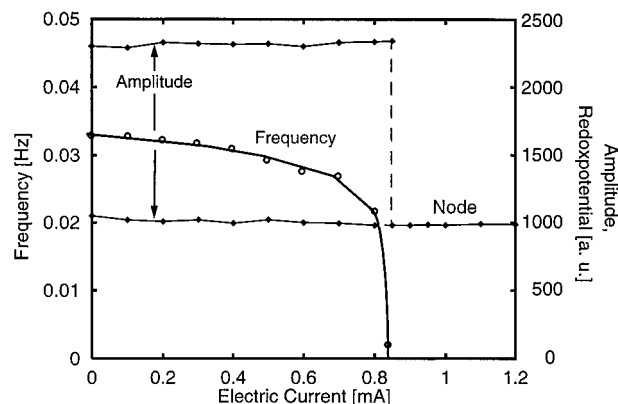

Figure 2. Experimental SNIPER scenario, electric current C as bifurcation parameter versus frequency (circles) and oscillation amplitude (diamonds); the SNIPER bifurcation occurs at 0.85 mA where the oscillation frequency is zero. The exitable node exists for $C > 0.85$ mA.

coupling equations are

$$G_1 = bias$$
$$G_2 = bias + w_{12} (Pot_1 - 1000)$$
$$G_3 = bias + w_{23} (Pot_2 - 1000) \qquad (1)$$
$$G_4 = bias + w_{34} (Pot_3 - 1000)$$

The bias (1.2 mA) and the coupling weights w_{ij} (-1.0 μA) are held constant. There will be no coupling contribution if the i-th CSTR is in a node, since ($Pot_i - 1000$) = 0. Otherwise, the coupling contributions are finite; that is, w_{ij} ($Pot_i - 1000 \neq 0$) for the coupling of reactor i with reactor j. To apply the first stimulus to the i-th CSTR, the electric current (bias) is switched off for $\sim$8 s. For shorter perturbations, no spike is generated. The arrows in the figures indicate the start of the 8 s stimulus.

When the first reactor (CSTR 1) is stimulated (perturbed) by a (negative) current pulse, a broad action potential (spike) is produced that induces consecutive spikes in the following reactors (CSTR 2, 3, and 4) (Figure 3 a). There are delays of about 10–15 s between the consecutive action potentials. Almost the same behavior can be observed by simultaneously perturbing two reactors (CSTR 1 and 4) which are separated by two reactors in-between (Figure 3b). In the last reactor (CSTR 4), two spikes appear, i.e., the second spike is generated from CSTR 3, since the initially stimulated CSTR 4 has already returned to its excitable steady state and its refractory time has passed.

When neighboring reactors (1 and 2) are perturbed synchronously, simultaneous action potentials are produced and the coupling between the two reactors has no effect (Figure 3c). The spikes in the other two reactors (CSTR 3 and 4) follow with the characteristic delay as in parts a and b of Figure 3.

After a simultaneous perturbation of nonadjacent reactors (CSTR 1 and CSTR 3) (Figure 3d), the spikes in the other two (CSTR 2 and CSTR 4) occur synchronously. Here, CSTR 3 is still in its refractory phase when the spike in CSTR 2 is produced. As a result, spike propagation stops here.
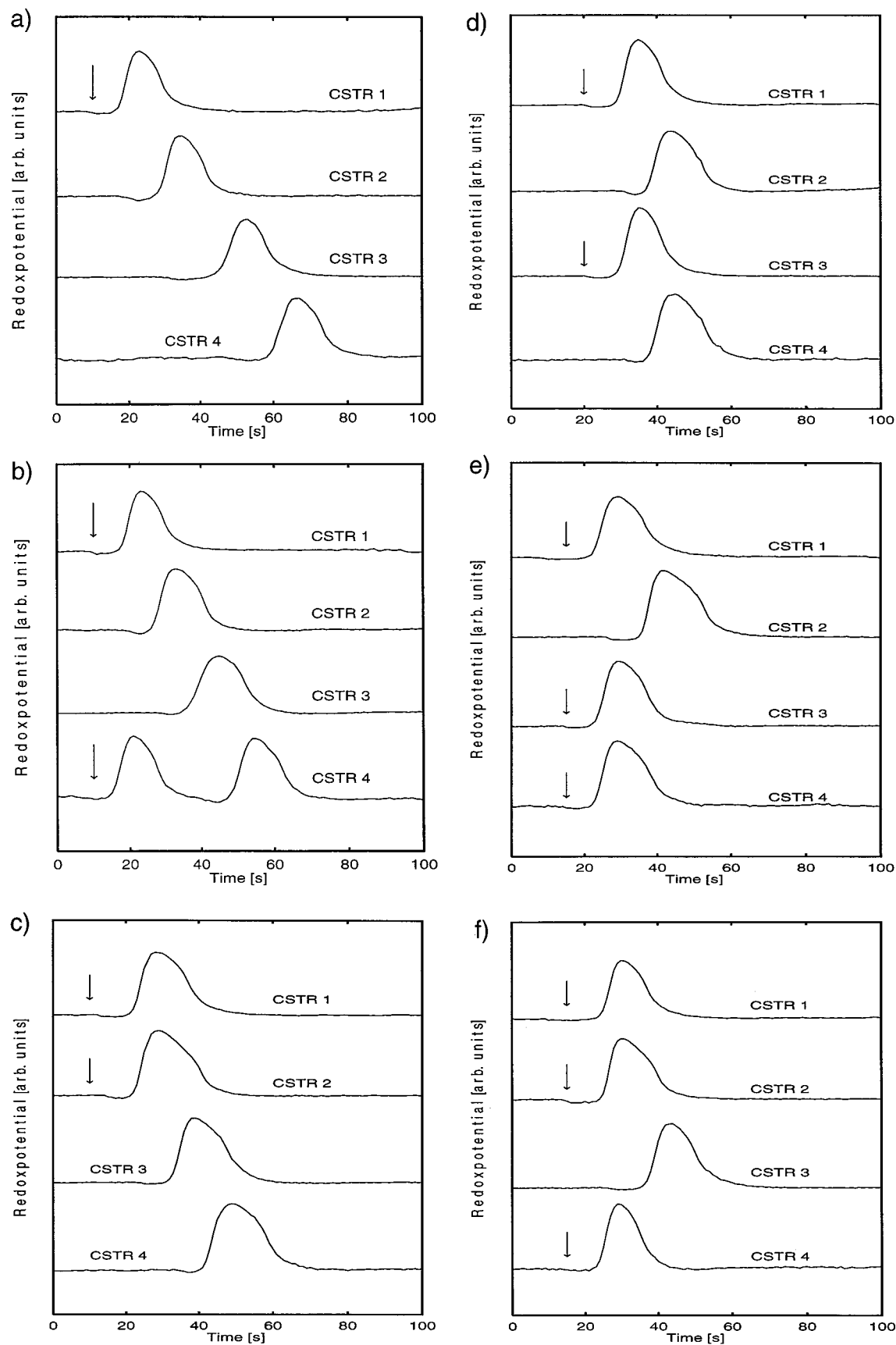
Figure 3. Linear coupling of four excitators where all reactors are in a nodal steady state (bias 1.2 mA); coupling weights $w_{ij} = -1.0$ μA, redox potential (arb. units) versus time. The following reactors are stimulated by an 8 s (negative) electric pulse (see arrow): (a) CSTR 1; (b) CSTR 1 and 4; (c) CSTR 1 and 2; (d) CSTR 1 and 3; (e) CSTR 1,3,4; (f) CSTR 1,2,4.

After simultaneous perturbations have been applied to three of the four reactors, the perturbed reactors respond with synchronous spikes while the spike in the externally nonperturbed reactor will follow with the characteristic delay (Figure
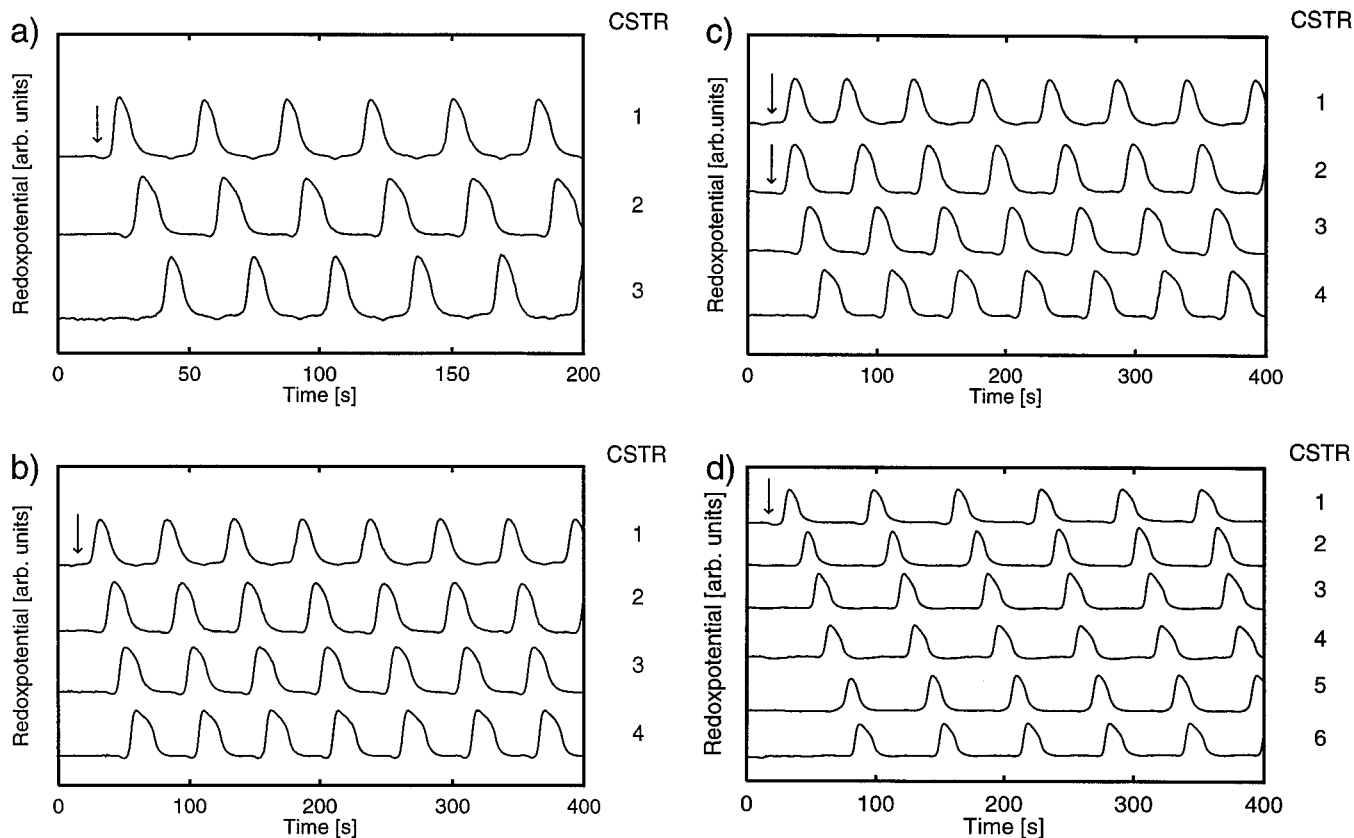
Electrically Coupled Chemical Oscillators

J. Phys. Chem. A, Vol. 103, No. 29, 1999 **5745**

Figure 4. Cyclic coupling of excitators: "traveling waves" of action potentials (for conditions see Figure 3): (a) three excitators; (b) four excitators; (c) four excitators where two neighboring excitators were simultaneously stimulated; (d) six excitators.

3e,f) provided the perturbed reactors include the first reactor; otherwise, there are only single spikes. If all four reactors are perturbed simultaneously, four synchronous spikes are produced with no following spikes. The linear coupling of an array of only two or three reactors can be easily derived by inspection (not shown) as a subset of the above four excitators.

Cyclic Coupling: Traveling Waves. *Three Excitators.* The intent here is to generate a self-sustaining "traveling wave". Due to the finite refractory time, at least three reactors are necessary which are coupled in a cyclic array:

$$G_1 = bias + w_{31} (Pot_3 - 1000)$$
$$G_2 = bias + w_{12} (Pot_1 - 1000) \qquad (2)$$
$$G_3 = bias + w_{23} (Pot_2 - 1000)$$
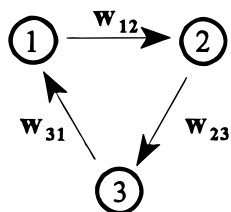
After perturbing any one of the three "excitators", a circulating "traveling wave" is generated (Figure 4a). A complete cycle, consisting of three action potentials, lasts about 32 s. A new wave of action potentials is started (by reactor 3), since the refractory time (of reactor 1) has elapsed. Thus, the rotating wave is sustained indefinitely. However, if any two reactors are simultaneously perturbed, spiking ceases after the first spike in this case.

Four Excitators. Using an array of four cyclically coupled reactors, a traveling wave is also generated if one reactor or two neighboring reactors are perturbed simultaneously (Figure 4b,c):

$$G_1 = w_{41} (Pot_4 - 1000) + bias$$
$$G_2 = w_{12} (Pot_1 - 1000) + bias$$
$$G_3 = w_{23} (Pot_2 - 1000) + bias \qquad (3)$$
$$G_4 = w_{34} (Pot_3 - 1000) + bias$$
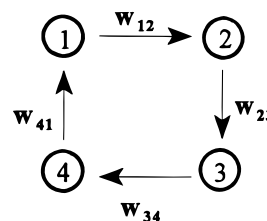
The resulting rotating waves are very stable. A complete cycle consists of four spikes, and it lasts somewhat longer (~50 s) than the previous cycle of three excitators. If two nonadjacent or three CSTRs are simultaneously perturbed, the response is similar to that of linear coupling as shown in parts d and e of Figure 3, where the propagation of spikes ceases due to blockage during the refractory time.

Six Excitators. Cyclic coupling of six reactors is shown in Figure 4d. In this particular experiment, the amplified redox potential of one reactor has been directly input into the galvanostat of the subsequent reactor without using the calculation of the difference $w_{ij}(Pot_i - 1000)$. Here, a single "round trip" consists of six spikes which takes about 60 s for the first
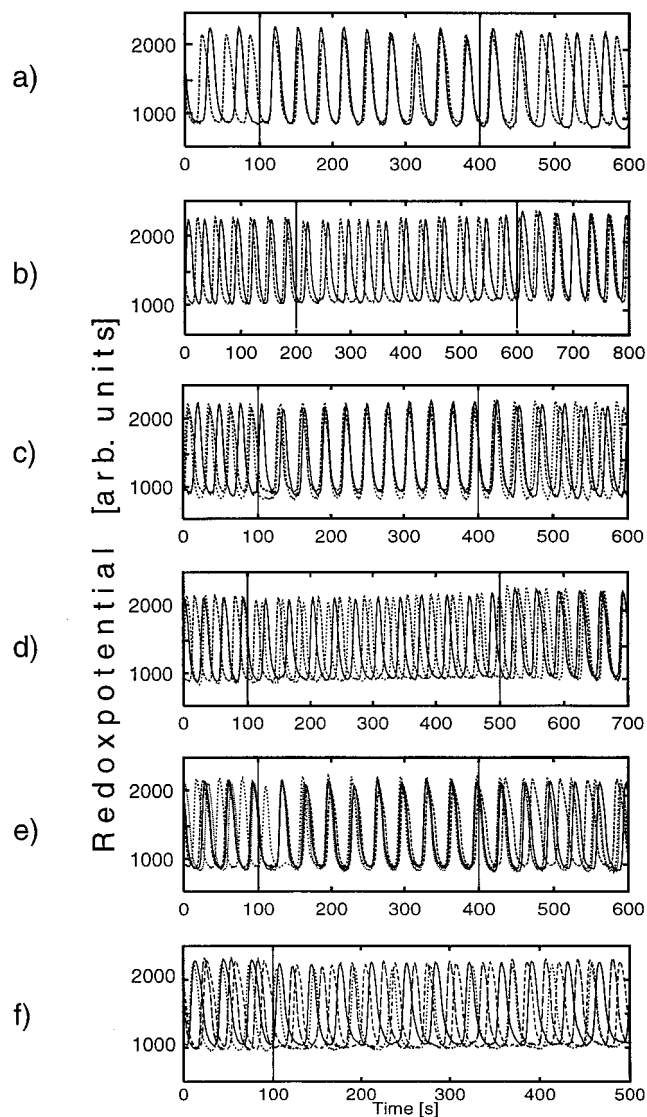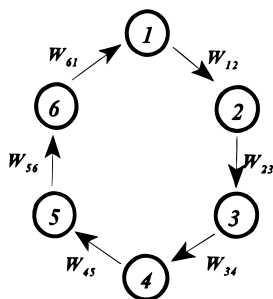
Figure 5. Phase behavior of mutually coupled oscillators, redox potential versus time; coupling is turned on and off (vertical lines): (a) two oscillators, $w_{ij} = -0.6$ μA, coherence; (b) two oscillators, $w_{ij} = 0.6$ μA, "bunching of phases"; (c) three oscillators, $w_{ij} = -0.4$ μA, coherence; (d) three oscillators, $w_{ij} = 0.4$ μA, ~120° out-of-phase motion; (e) four oscillators, $w_{ij} = -0.25$ μA, coherence; (f) four oscillators, $w_{ij} = 0.25$ μA, complex incoherence; reactor 1 (solid line), reactor 2 (small dashes), reactor 3 (points), reactor 4 (large dashes).

completion after which it continues indefinitely.

Phase Behavior of Two, Three, and Four Mutually Coupled Chemical Oscillators. *Two Oscillators.* In our experiments, we start with *two* oscillating reactors which are mutually

coupled according to

$$G_1 = w_{21} (Pot_2 - Pot_1)$$
$$G_2 = w_{12} (Pot_1 - Pot_2)$$
(4)

After the coupling interaction is turned on (at $T = 100$ s) with $w_{ij} = -0.6$ μA, synchronization is achieved rapidly within the first oscillation (Figure 5a). When the coupling is switched off after 300 s, the two free running oscillators eventually loose their coherence due to small differences in their frequencies. However, when the coupling interaction is positive, $w_{ij} = 0.6$ μA, the phenomenon of "bunching" of phases is observed; that is, the phase angle between the two oscillators is constant and always less than 180° (Figure 5b).

Three Oscillators. Mutual coupling of three chemical oscillators rapidly produces coherence ($w_{ij} = -0.4$ μA) within ~2 oscillations (Figure 5c), whereas positive coupling ($w_{ij} = 0.4$ μA) leads to an out-of-phase motion (Figure 5d) of approximately 120°.

$$G_1 = w_{21} (Pot_2 - Pot_1) + w_{31} (Pot_3 - Pot_1)$$
$$G_2 = w_{12} (Pot_1 - Pot_2) + w_{32} (Pot_3 - Pot_2)$$
$$G_3 = w_{13} (Pot_1 - Pot_3) + w_{23} (Pot_2 - Pot_3)$$
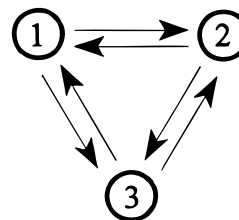
(5)

Four Oscillators. When *four* chemical oscillators are mutually coupled *with* $w_{ij} = -0.25$ μA (Figure 5e), coherent motion occurs almost as rapidly as in the previous case for three reactors. When the coupling strength is positive ($w_{ij} = 0.25$ μA), a complex exchange of phases takes place with time (Figure 5f), in contrast to the case of three coupled oscillators (Figure 5d), where about 120° out-of-phase motion occurs.
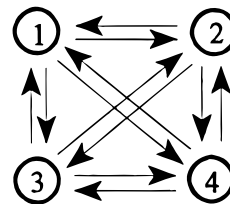
Numerical Simulations

To simulate the present experiments, we use the seven-variables Montanator model by Györgyi and Field.[17] The model uses two autocatalytic cycles, one describing the production of $HBrO_2$ by the reduction of bromate with Ce^{3+} and the other the formation of Br^- from bromomalonic acid as the autocatalytic species. The mechanism is given in Table 1, and the rate constants and concentrations of the in-flow species are given in Table 2. The seven variables are bromous acid, bromide, bromate, bromomalonic acid, bromomalonic acid radical, Ce^{3+}, and Ce^{4+}. Numerical integrations were done with the Gear method.[18] The effect of the electric current enters into the

Electrically Coupled Chemical Oscillators

J. Phys. Chem. A, Vol. 103, No. 29, 1999 **5747**

TABLE 1: Seven-Variables Model (Nonstoichiometric Steps)

$Br^- + HBrO_2 + H^+$	$\rightarrow$	$2BrMA$	(R1)
$Br^- + BrO_3^- + 2H^+$	$\rightarrow$	$BrMA + HBrO_2$	(R2)
$2HBrO_2$	$\rightarrow$	$BrO_3^- + BrMA + H^+$	(R3)
$BrO_3^- + HBrO_2 + H^+$	$\rightarrow$	$2BrO_2^\bullet + H_2O$	(R4)
$2BrO_2^\bullet + H_2O$	$\rightarrow$	$BrO_3^- + HBrO_2 + H^+$	(R5)
$Ce^{3+} + BrO_2^\bullet + H^+$	$\rightarrow$	$HBrO_2 + Ce^{4+}$	(R6)
$HBrO_2 + Ce^{4+}$	$\rightarrow$	$Ce^{3+} + BrO_2^\bullet + H^+$	(R7)
$MA + Ce^{4+}$	$\rightarrow$	$MA^\bullet + Ce^{3+} + H^+$	(R8)
$BrMA + Ce^{4+}$	$\rightarrow$	$Ce^{3+} + Br^-$	(R9)
$MA^\bullet + BrMA$	$\rightarrow$	$MA + Br^-$	(R10)
$2MA^\bullet$	$\rightarrow$	MA	(R11)

MA = malonic acid; $MA^\bullet$ = malonic acid radical;
BrMA = bromomalonic acid;

TABLE 2: Rate Constants and Concentrations of the Seven-Variables Model

k_{R1}	$2.0 \times 10^6 \text{ s}^{-1} \text{ M}^{-1}$	k_{R2}	$2.0 \text{ s}^{-1} \text{ M}^{-3}$
k_{R3}	$3.0 \times 10^3 \text{ s}^{-1} \text{ M}^{-1}$	k_{R4}	$3.3 \times 10^1 \text{ s}^{-1} \text{ M}^{-2}$
k_{R5}	$7.6 \times 10^5 \text{ s}^{-1} \text{ M}^{-2}$	k_{R6}	$6.2 \times 10^4 \text{ s}^{-1} \text{ M}^{-2}$
k_{R7}	$7.0 \times 10^3 \text{ s}^{-1} \text{ M}^{-1}$	k_{R8}	$3.0 \times 10^{-1} \text{ s}^{-1} \text{ M}^{-1}$
k_{R9}	$3.0 \times 10^1 \text{ s}^{-1} \text{ M}^{-1}$	k_{R10}	$2.4 \times 10^4 \text{ s}^{-1} \text{ M}^{-1}$
k_{R11}	$3.0 \times 10^9 \text{ s}^{-1} \text{ M}^{-1}$		
$[BrO_3^-]$	0.1 M	$[H^+]$	0.26 M
$[H_2O]$	55 M	$[Ce^{3+}]_0$	8.33×10^{-4} M
$[MA]$	0.25 M		

differential equations by adding $C[Ce^{4+}]$ to the rate equation for $[Ce^{3+}]$ and by subtracting the term $C[Ce^{4+}]$ from the rate equation of $[Ce^{4+}]$:

$$\frac{d[Ce^{3+}]}{dt} = f([Ce^{3+}]) - k_f([Ce^{3+}] - [Ce^{3+}]_0) + C[Ce^{4+}]$$

$$\frac{d[Ce^{4+}]}{dt} = f([Ce^{4+}]) - k_f[Ce^{4+}] - C[Ce^{4+}]$$

where C is a rate parameter for a reactor proportional to the amount of charge delivered at the Pt-working electrode, $[Ce^{3+}]_0$ is the inflow concentration of Ce^{3+} (Table 2) and $f([Ce^{3+}])$ contains the respective rate equation for the model (Table 1). For an individual reactor i, C is written as C_i, where C_i is equal to G_i (electric current in reactor i) as given in the respective coupling equations (see above). To obtain free running period-one oscillations for $C = 0$, a flow rate of $k_f = 3.5 \times 10^{-4} \text{ s}^{-1}$ was chosen. In the absence of coupling, a SNIPER bifurcation is obtained at $C = 0.11$ as recently described.[11] For values of C above 0.11, a nodal steady-state exists, whereas for C between 0 and 0.11, P_1 chemical oscillations are observed.[11]

The results of the simulations are given for wave propagation in four excitators which are linearly (Figure 6a) and cyclically (Figure 6b) coupled. Linear coupling (Figure 6a) also produces a transitory overshoot of $[Ce^{4+}]$ which is not observed in the experiments. Cyclic coupling (Figure 6b) shows a relatively long transience ($\sim$800 s) in the model calculations in the absence of additive noise. Notice that the calculated $[Ce^{4+}]$ concentrations are "inverted" with respect to the experimental potentials due to the fact that the level of the nodal steady state is somewhat higher than the minima of the P_1 oscillations.[11,12] On the other hand, in the experiments, these levels are practically equal (Figure 2). In general, only a fair agreement is obtained between the simulations and the experiments. This also applies to the simulations of the phase behavior (Figure 7a), where, for negative values of the coupling strength, coherence between three mutually coupled oscillators is reached after a transience,
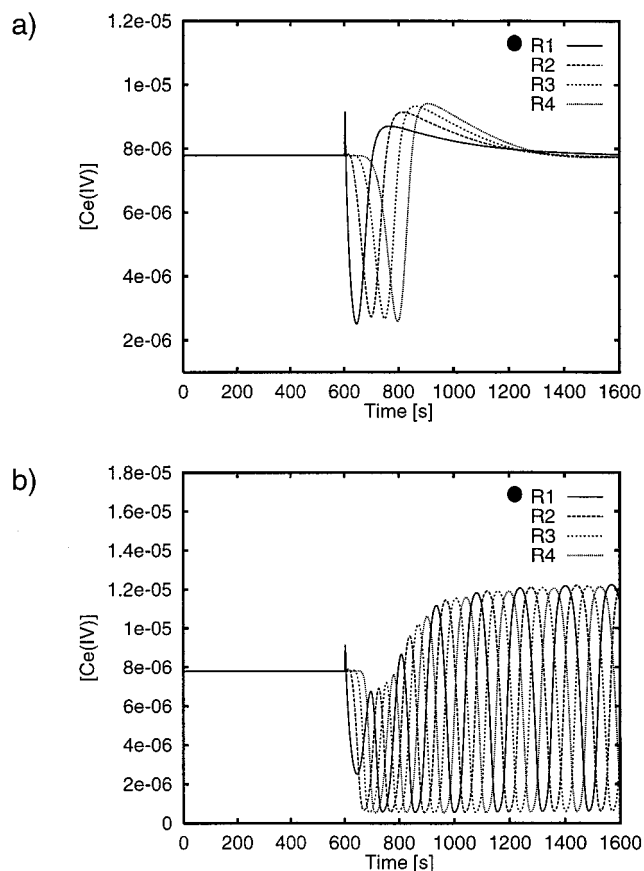

Figure 6. Calculated time series of four coupled excitators for (a) unidirectional coupling and (b) cyclic coupling. A short pulse is applied to excitator 1 (R1) at $t = 600$ s, $w_{ij} = 1150$ (arb. units)
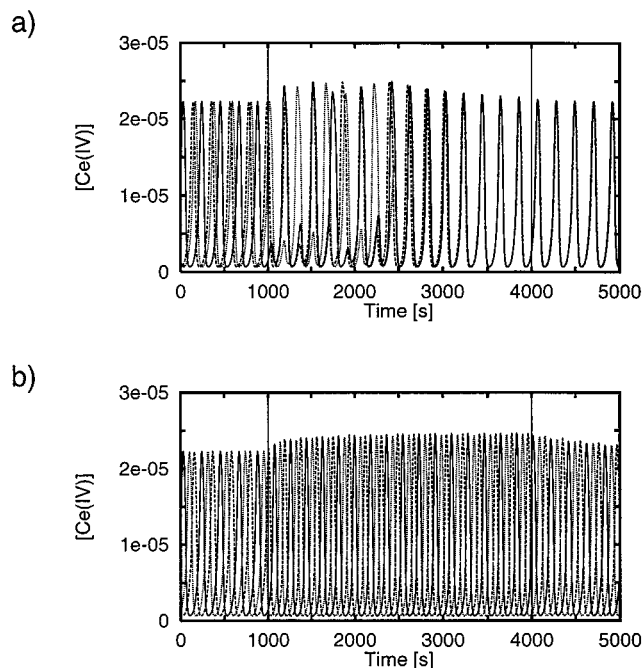

Figure 7. Calculated time series of three mutually coupled oscillators; oscillator 1 (solid line), oscillator 2 (small dashes), oscillator 3 (points); coupling is active between $t = 1000$ s and $t = 4000$ s (vertical lines): (a) $w_{ij} = -110$ (arb. units), coherence starting at $\sim$3000 s; (b) $w_{ij} = 110$ (arb. units), $\sim$120° out-of-phase motion.

which is longer than that in the experiments. For intermediate positive coupling strengths, the electrically coupled oscillators are $\sim$120° out-of-phase as in the experiments (Figure 7b).

Further numerical calculations will be carried out which take various initial conditions (phases, start of coupling), coupling strengths, and interactive noise into account.

The Effect of Coupling Strength. A minimum coupling strength is necessary to achieve synchronization which depends on the number of reactors. Generally speaking, the larger the reactor network the smaller is the coupling strength necessary for synchronization.

Discussion

In our present experiments, we use a Pt-working electrode in a BZ-reactor in which the external electrical current converts Ce^{4+} to Ce^{3+} at the redox electrode as the main process.[11,12] The electric current operates in a similar fashion as the addition of a aliquot of a Ce^{4+} solution as shown by measurements of identical phase response curves.[19] Generally speaking, the effect of an electric current on redox processes at the Pt-working electrode will be different for different oscillating reactions. However, the same generic behavior is likely to be observed by either a cathodic or an anodic current in any chemical oscillator that involves redox processes if the electrical current is a bifurcation parameter.

Our experiments show the occurrence of "traveling (rotating) waves" of action potentials for the first time in a cyclic array of BZ-excitators. Due to the finite refractory time, a minimum number of coupled excitators are required, namely, three in this case, to achieve a sustained rotatory wave. More than 100 rounds (over 400 action potentials) have been recorded before the experiment was arbitrarily stopped. Electrical coupling may also be carried out without the use of a computer by using the amplified redox potential of the Pt|Ag|AgCl monitoring electrode as a direct input to the galvanostat, which delivers the electric current to the Pt-working electrodes.

Our present experiments also support the general notion that, in mutually coupled chemical oscillators, in-phase coherence is the rule rather than the exception. This is true only if the oscillators are coupled via attractive interactions, as given by the negative sign of the coupling constant w_{ij} in this case. Furthermore, the variance of the frequencies of the free running oscillators should be sufficiently small, and the coupling interactions should not be too large. The larger the number of mutually coupled chemical oscillators, the smaller the attractive coupling strength w_{ij} has to be. In general, coherence is attained during the first or second oscillation depending on initial conditions independently of the number of the mutually coupled reactors. Unidirectional (as well as mutual) coupling is also expected to lead to coherent motion if the number of oscillators in a cyclic array is small ($\lesssim$4). Interestingly, the out-of-phase motion (for $w_{ij} > 0$) is stable only for small reactor arrays, i.e., two to three reactors for repulsive coupling, whereas for mass coupling, out-of-phase behavior seems to be a transient phenomenon only.

When the coupling interaction is turned off, coherence disappears due to small differences in the individual oscillator frequencies and due to the ever-present noise. In fact, our numerical simulations of the seven-variables Montanator show that noise must be added to convert a stable 180°-out-of-phase motion into an in-phase motion.

Numerical simulations of the present chemical reaction model show only fair agreement with the experiments; the level of the nodal steady state (Ce^{4+}) at high currents is higher in the simulations[11,12] than in the experiment (Figure 2). This leads to action potentials that appear to be inverted with respect to the experimental behavior. The general phase behavior of the electrically coupled oscillators will be further investigated by numerical simulations.

References and Notes

(1) Strogatz, S. H.; Stewart, I. *Sci. Am.* **1993**, 68.

(2) Collins, J. J.; Stewart, I. *J. Nonl. Sci.* **1993**, *3*, 349.

(3) MacLeod, K.; Laurent, G. *Science* **1996**, *274*, 976.

(4) Marek, M.; Stuchl, I. *Biophys. Chem.* **1975**, *3*, 241. Nakajima, K.; Sawada, Y. *J. Chem. Phys.* **1980**, *72*, 2231. Stuchl, I.; Marek, M. *J. Chem. Phys.* **1982**, *77*, 1697. Bar-Eli, K. *J. Phys. Chem.* **1984**, *88*, 3616. Bar-Eli, K.; Reuveni, S. *J. Phys. Chem.* **1985**, *89*, 1329. Boukalouch, M.; Elezgaray, J.; Arneodo, A.; Boissonade, J.; De Kepper, P. *J. Phys. Chem.* **1987**, *91*, 5843. Crowley, M.; Epstein, I. R. *J. Phys. Chem.* **1989**, *93*, 2496. Yosimoto, M.; Yoshikawa, K.; Mori, Y.; Hanazaki, I. *Chem. Phys. Lett.* **1992**, *189*, 18. Doumbouya, S. I.; Münster, A. F.; Doona, C. J.; Schneider, F. W. *J. Phys. Chem.* **1993**, *97*, 1025. Doumbouya, S. I.; Schneider, F. W. *J. Phys. Chem.* **1993**, *97*, 6945. Hauser, M. J. B.; Schneider, F. W. *J. Chem. Phys.* **1994**, *100*, 1058. Lekebusch, A.; Schneider, F. W. *J. Phys. Chem.* **1997**, *101*, 9838.

(5) Laplante, J.-P.; Erneux, T. *J. Phys. Chem.* **1992**, *96*, 4931. Booth, V.; Erneux, T.; Laplante, J.-P. *J. Phys. Chem.* **1994**, *98*, 6537. Laplante, J.-P.; Pemberton, M.; Hjelmfelt, A.; Ross, J. *J. Phys. Chem.* **1995**, *99*, 10063.

(6) Zhabotinsky, A. M.; Zaikin, A. N.; Rovinskii, A. B. *React. Kinet. Catal. Lett.* **1982**, *20*, 29. Weiner, J.; Schneider, F. W.; Bar-Eli, K. *J. Phys. Chem.* **1989**, *93*, 2704. Chevalier, T.; Freund, A.; Ross, J. *J. Chem. Phys.* **1991,** *95*, 308. Roesky, P. W.; Doumbouya, S. I.; Schneider, F. W. *J. Phys. Chem.* **1992**, *96*, 8915. Holz, R.; Schneider, F. W. *J. Phys. Chem.* **1993**, *97*, 12239. Zeyer, K.-P.; Holz, R.; Schneider, F. W. *Ber. Bunsen-Ges. Phys. Chem.* **1993**, *97*, 1112. Yoshimoto, M.; Yoshikawa, K.; Mori, Y. *Phys. Rev. E* **1993**, *47*, 864.

(7) Hohmann, W.; Kraus, M.; Schneider, F. W. *J. Phys. Chem. A* **1998**, *102*, 3103.

(8) Crowley, M. F.; Field, R. J. In *Nonlinear Phenomena in Chemical Dynamics*; Vidal, C., Pacault, A., Eds.; Springer: Berlin, 1981; p 147. Crowley, M. F.; Field, R. J. In *Lecture Notes in Biomathematics, Nonlinear Oscillations in Biology and Chemistry*; Othmer, H., Ed.; Springer: Berlin, 1986; p 68. Crowley, M. F.; Field, R. J. *J. Phys. Chem.* **1986**, *90*, 1907. Botré, C.; Lucarini, C.; Memoli, A.; D'Ascenzo, E. *Bioelectrochem. Bioenerg.* **1981**, *8*, 201. Schneider, F. W.; Hauser, M. J. B.; Reising, J. *Ber. Bunsen-Ges. Phys. Chem.* **1993**, *97*, 55. Zeyer, K.-P.; Münster, A. F.; Hauser, M. J. B.; Schneider, F. W. *J. Chem. Phys.* **1994**, *101*, 5126.

(9) Zeyer, K.-P.; Dechert, G.; Hohmann, W.; Schneider, F. W. *Z. Naturforsch.* **1994**, *49A*, 383.

(10) Dechert, G.; Zeyer, K.-P.; Lebender, D.; Schneider, F. W. *J. Phys. Chem.* **1996**, *100*, 19043.

(11) Hohmann, W.; Kraus, M.; Schneider, F. W. *J. Phys. Chem.* **1997**, *101*, 7364.

(12) Hohmann, W.; Kraus, M.; Schneider, F. W. *J. Phys. Chem. A* **1998**, *102*, 3103.

(13) Marek, M.; Schreiber, I. Chaos in Forced and Coupled Oscillators and Exitators. In *Chaos in Chemistry and Biochemistry*; Field, R. J., Györgyi, L., Eds.; World Scientific: Singapore; 1993; p 87. Dolník, M.; Finkeová, J.; Schreiber, I.; Marek, M. *J. Phys. Chem.* **1989**, *93*, 2764. Finkeová, J.; Dolník, M.; Hrudka, B.; Marek, M. *J. Phys. Chem.* **1990**, *94*, 4100. Kosek, J.; Schreiber, I.; Marek, M. *Philos. Trans. R. Soc. London, Ser. A* **1994**, *347*, 643. Dolník, M.; Marek, M. *J. Phys. Chem.* **1991**, *95*, 7262. Dolník, M.; Marek, M.; Epstein, I. R. *J. Phys. Chem.* **1992**, *96*, 3218. Dolník, M.; Kosek, J.; Votrubová, V.; Marek, M. *J. Phys. Chem.* **1994**, *98*, 3707.

(14) Nevoral, V.; Votrubová, V.; Hasal, P.; Schreiberová, L.; Marek, M. *J. Phys. Chem. A* **1997**, *101*, 4954. Votrubová, V.; Hasal, P.; Schreiberová, L.; Marek, M. *J. Phys. Chem.* **1998**, *102*, 1318.

(15) Schneider, F. W.; Münster, A. F. *J. Phys. Chem.* **1991**, *95*, 2130.

(16) Noszticzius, Z.; Wittmann, M.; Stirling, P. *J. Phys. Chem.* **1985**, *89*, 4914. Noszticzius, Z.; Wittmann, M.; Stirling, P. *J. Chem. Phys.* **1987,** *86*, 1922.

(17) Györgyi, L.; Field, R. J. *J. Phys. Chem.* **1991**, *95*, 6594. Györgyi, L.; Field, R. J. *Nature* **1992**, *355*, 808.

(18) Gear, C. W. *Numerical Initial Value Problems in Ordinary Differential Equations*; Prentice Hall: Englewood Cliffs, NJ, 1971.

(19) Dechert, G.; Lebender, D.; Schneider, F. W. *J. Phys. Chem.* **1995**, *99*, 11432.